

Electronic Supplementary Information (ESI):

Interplay of Alternative Conjugated Pathways and Steric Interactions on the Electronic and Optical Properties of Donor-Acceptor Conjugated Polymers

**Igo T. Lima,^{1,2} Chad Risko,^{1,†,*} Saadullah G. Aziz,³
Demétrio A. da Silva Filho,^{2,*} and Jean-Luc Brédas^{1,3,‡,*}**

¹ School of Chemistry and Biochemistry and Center for Organic Photonics and Electronics
Georgia Institute of Technology
Atlanta, Georgia, 30332-0400, United States of America

² Institute of Physics, University of Brasilia, 70919-970, Brasilia, Brazil

³ Department of Chemistry, King Abdulaziz University, Jeddah 21589, Kingdom of Saudi Arabia

[†]*New Permanent Address:* Department of Chemistry, University of Kentucky, Lexington, Kentucky, 40506, USA

[‡]*New Permanent Address:* Physical Sciences and Engineering Division, King Abdullah University of Science and Technology (KAUST), Thuwal 23955-6900, Kingdom of Saudi Arabia

List of Tables & Figures.

Table S1. Optimized range-separation parameter (ω) as determined via gap-fitting at the tuned-LC-BLYP/6-31G(d,p) level of theory (1 bohr = 0.529 Å).

Table S2. HOMO and LUMO energies and HOMO-LUMO gap (E_{gap}) as determined with either the tuned-LC-BLYP or B3LYP functional and the 6-31G(d,p) basis set.

Figure S1. Illustration of representative tetramer frontier molecular orbitals determined at the tuned-LC-BLYP/6-31G(d,p) level of theory.

Table S3. PbTBT and PbTTP $S_0 \rightarrow S_1$ vertical transition energies (E_{01}) and wavelengths (λ_{01}), oscillator strengths (f), transition dipole moments (μ_{01}), and electronic configurations as determined with TDDFT at the tuned-LC-BLYP/6-31G(d,p) level of theory.

Table S4. PCzBT and PCzTP $S_0 \rightarrow S_1$ vertical transition energies (E_{01}) and wavelengths (λ_{01}), oscillator strengths (f), transition dipole moments (μ_{01}), and electronic configurations as determined with TDDFT at the tuned-LC-BLYP/6-31G(d,p) level of theory.

Table S5. PCzTh-TVDCN and PTh-TVDCN $S_0 \rightarrow S_1$ vertical transition energies (E_{01}) and wavelengths (λ_{01}), oscillator strengths (f), transition dipole moments (μ_{01}), and electronic configurations as determined with TDDFT at the tuned-LC-BLYP/6-31G(d,p) level of theory.

Figure S2. Absolute values of $S_0 \rightarrow S_1$ transition dipole moment as determined with TDDFT at the tuned-LC-BLYP/6-31G(d,p) level of theory.

Figure S3. Natural transition orbitals (NTO) describing the $S_0 \rightarrow S_1$ transition for the linear copolymers as determined with TDDFT at the tuned LC-BLYP/6-31G(d,p) level of theory.

Figure S4. Natural transition orbitals (NTO) describing the $S_0 \rightarrow S_1$ transition for the orthogonally conjugated copolymers as determined with TDDFT at the tuned LC-BLYP/6-31G(d,p) level of theory.

Figure S5. Evolution of the HOMO (top) and LUMO (bottom) energies (eV) with respect to the inverse number of repeat units (n) in the oligomer as determined at the B3LYP/6-31G(d,p) level of theory.

Figure S6. Evolution of the $S_0 \rightarrow S_1$ vertical transition energy (top) and absolute value of the transition dipole moment (bottom) with respect to the inverse number of repeat units ($1/n$), as calculated with TDDFT at the B3LYP/6-31G(d,p) level of theory.

Figure S7. UV-visible absorption spectra of the PCzTh-TVDCN calculated at the B3LYP (red) and tuned-LC-BLYP (blue) both with the 6-31G(d,p) basis set.

Table S1. Optimized range-separation parameter (ω) as determined via gap-fitting at the tuned-LC-BLYP/6-31G(d,p) level of theory (1 bohr = 0.529 Å).

		n	ω (bohr ⁻¹)
Linear	PbTBT	1	0.222
		2	0.165
		3	0.142
		4	0.132
	PbTTP	1	0.217
		2	0.155
		3	0.126
		4	0.110
	PCzBT	1	0.223
		2	0.177
		3	0.168
		4	0.167
	PCzTP	1	0.215
		2	0.161
		3	0.146
		4	0.140
Orthogonal	PCzTh-TVDCN	1	0.199
		2	0.169
		3	0.160
		4	0.159
	PTTh-TVDCN	1	0.195
		2	0.168
		3	0.164
		4	0.164

Table S2. HOMO and LUMO energies and HOMO-LUMO gap (E_{gap}) as determined with either the tuned-LC-BLYP or B3LYP functional and the 6-31G(d,p) basis set.

			HOMO	LUMO	E_{gap}
tuned-LC-BLYP (B3LYP)	Linear	PbTBT	-5.64 (-4.85)	-1.85 (-3.00)	3.79 (1.84)
		PbTTP	-5.05 (-4.47)	-2.05 (-3.03)	3.00 (1.43)
		PCzBT	-6.25 (-5.13)	-1.12 (-2.47)	5.13 (2.65)
		PCzTP	-5.57 (-4.69)	-1.45 (-2.61)	4.11 (2.07)
	Orthogonal	PCzTh-TVDCN	-6.08 (-5.25)	-2.17 (-3.22)	3.91 (2.03)
		PTTh-TVDCN	-5.91 (-4.95)	-1.90 (-3.24)	4.01 (1.70)

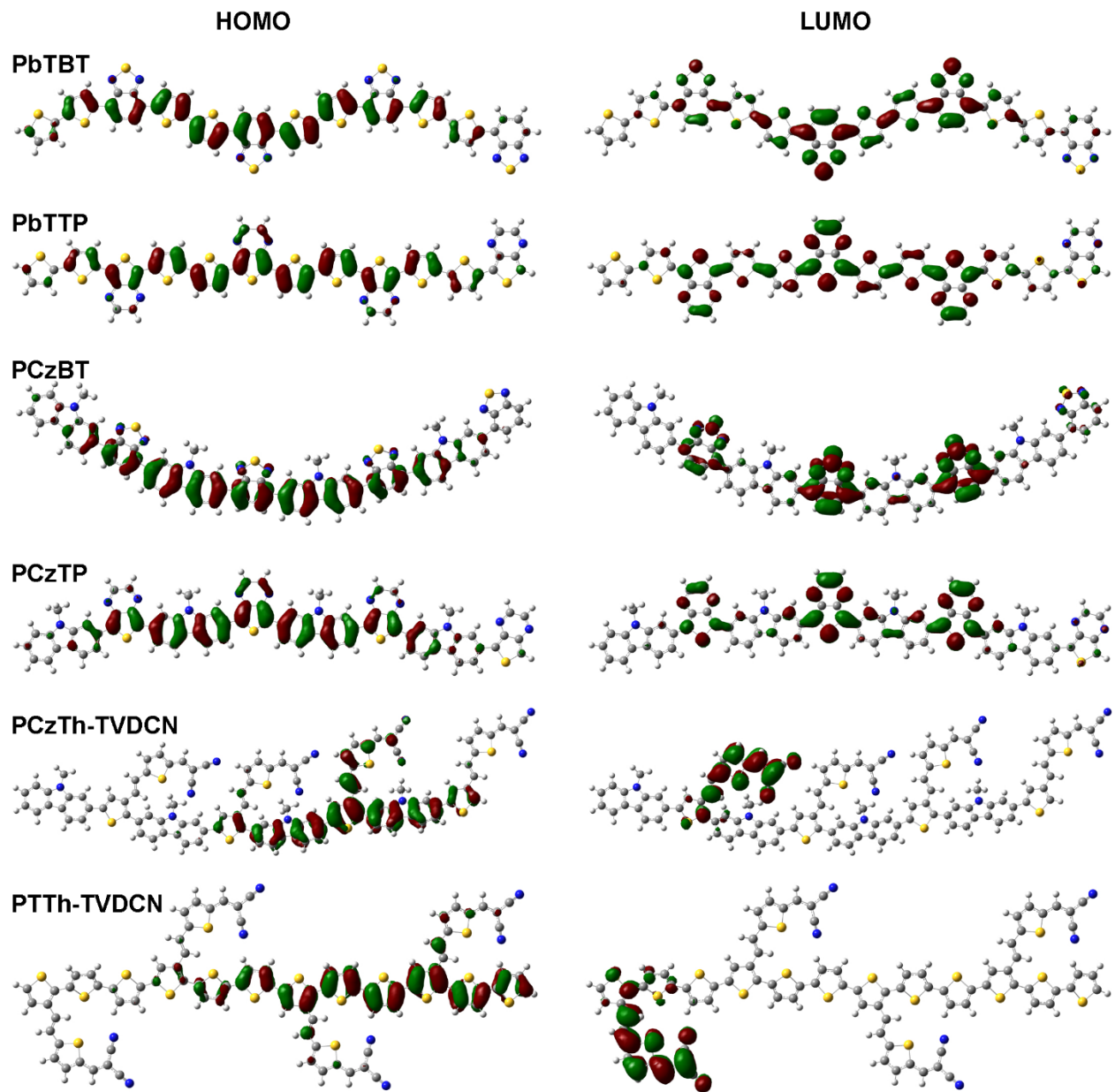


Figure S1. Illustration of representative tetramer frontier molecular orbitals determined at the tuned-LC-BLYP/6-31G(d,p) level of theory.

Table S3. PbTBT and PbTTP $S_0 \rightarrow S_1$ vertical transition energies (E_{01}) and wavelengths (λ_{01}), oscillator strengths (f), transition dipole moments (μ_{01}), and electronic configurations as determined with TDDFT at the tuned-LC-BLYP/6-31G(d,p) level of theory.

	n	E_{01} (eV)	λ_{01} (nm)	F	μ_{01} (Debye)				Electronic Configuration(%)
					x	Y	Z	Total	
PbTBT	1	3.09	400	0.45	-6.19	-0.01	0.02	6.19	HOMO-1→LUMO(5) HOMO→LUMO(89)
	2	2.19	563	1.08	11.36	-0.31	0.00	11.37	HOMO-1→LUMO+1(3) HOMO→LUMO(86) HOMO→LUMO+1(3)
	3	1.90	651	2.04	-16.81	0.13	0.07	16.81	HOMO-1→LUMO+1(14) HOMO→LUMO(75)
	4	1.76	702	3.00	-21.15	0.42	-0.13	21.16	HOMO-2→LUMO+2(6) HOMO-1→LUMO+1(17) HOMO→LUMO(66)
PbTTP	1	2.71	457	0.33	-5.64	0.98	-0.02	5.72	HOMO-1→LUMO(6) HOMO→LUMO(91)
	2	1.78	694	0.92	-11.64	-0.41	0.0	11.65	HOMO-1→LUMO+1(3) HOMO→LUMO(87) HOMO→LUMO+1(3)
	3	1.47	844	1.83	18.15	-0.30	-0.08	18.15	HOMO-1→LUMO+1(13) HOMO→LUMO(80)
	4	1.28	966	2.77	-23.88	-0.15	-0.01	23.88	HOMO-2→LUMO+2(4) HOMO-1→LUMO+1(15) HOMO→LUMO(74)

Table S4. PCzBT and PCzTP $S_0 \rightarrow S_1$ vertical transition energies (E_{01}) and wavelengths (λ_{01}), oscillator strengths (f), transition dipole moments (μ_{01}), and electronic configurations as determined with TDDFT at the tuned-LC-BLYP/6-31G(d,p) level of theory.

	n	E_{01} (eV)	λ_{01} (nm)	f	μ_{01} (Debye)				Electronic Configuration(%)
					x	y	Z	Total	
PCzBT	1	3.47	357	0.31	-4.79	-0.75	0.01	4.85	HOMO-2→LUMO(15) HOMO-1→LUMO(77) HOMO→LUMO(4)
	2	2.78	446	0.78	8.60	0.0	0.15	8.60	HOMO-4→LUMO(3) HOMO-4→LUMO+1(2) HOMO-3→LUMO+1(2) HOMO→LUMO(74) HOMO→LUMO+1(11)
	3	2.65	467	1.55	-12.43	0.40	-0.07	12.44	HOMO-6→LUMO+1(2) HOMO-6→LUMO+2(2) HOMO-3→LUMO+1(2) HOMO-2→LUMO+1(6) HOMO-1→LUMO+1(6) HOMO→LUMO (61) HOMO→LUMO+1(2)
	4	2.61	475	2.24	-15.05	0.60	-0.11	15.06	HOMO-8→LUMO+3(2) HOMO-6→LUMO+2(8) HOMO-1→LUMO+1(18) HOMO→LUMO(51) HOMO→LUMO+1(2)
PCzTP	1	2.89	429	0.26	4.79	0.86	0.07	4.87	HOMO-2→LUMO(8) HOMO→LUMO(87)
	2	2.12	585	0.67	-9.18	-0.10	0.23	9.18	HOMO-3→LUMO(2) HOMO-3→LUMO+1(2) HOMO→LUMO(79) HOMO→LUMO+1(7)
	3	1.95	635	1.46	14.06	-0.18	-0.02	14.06	HOMO-5→LUMO+2(2) HOMO-1→LUMO+1(19) HOMO-1→LUMO+2(2) HOMO→LUMO(67)
	4	1.87	661	2.23	-17.73	0.18	-0.03	17.74	HOMO-2→LUMO+2(10) HOMO-1→LUMO+1(19) HOMO→LUMO(58)

Table S5. PCzTh-TVDCN and PTTh-TVDCN $S_0 \rightarrow S_1$ vertical transition energies (E_{01}) and wavelengths (λ_{01}), oscillator strengths (f), transition dipole moments (μ_{01}), and electronic configurations as determined with TDDFT at the tuned-LC-BLYP/6-31G(d,p) level of theory.

	n	E_{01} (eV)	λ_{01} (nm)	f	μ_{01} (Debye)				Electronic Configuration(%)
					X	y	z	Total	
PCzTh-TVDCN	1	2.97	417	1.25	8.70	5.92	0.41	10.53	HOMO-2→LUMO(31) HOMO→LUMO(63)
	2	2.43	508	0.30	1.53	4.66	2.89	5.70	HOMO-5→LUMO(12) N2HOMO-1→LUMO(9) HOMO→LUMO(70)
	3	2.21	558	0.14	2.39	3.00	1.53	4.13	HOMO-8→LUMO(7) HOMO-3→LUMO(17) HOMO-2→LUMO(4) HOMO-1→LUMO(27) HOMO→LUMO(36)
	4	2.19	563	0.10	2.61	2.43	0.54	3.61	HOMO-11→LUMO(6) HOMO-5→LUMO(30) HOMO-3→LUMO(3) HOMO-2→LUMO(4) HOMO-1→LUMO(38) HOMO-1→LUMO+1(2) HOMO→LUMO(6)
PTTh-TVDCN	1	2.54	487	0.34	-0.99	5.88	-0.20	5.96	HOMO-1→LUMO(10) HOMO→LUMO(79) HOMO→LUMO+1(6)
	2	2.25	550	0.38	1.63	6.47	-0.43	6.69	HOMO-2→LUMO+1(2) HOMO-1→LUMO+1(9) HOMO→LUMO+1(76) HOMO→LUMO+3(2)
	3	2.16	574	0.45	-4.88	5.55	-0.61	7.42	HOMO-2→LUMO+1(10) HOMO-1→LUMO+1(15) HOMO→LUMO+1(56) HOMO→LUMO+3(4) HOMO→LUMO+4(2)
	4	2.14	577	0.47	-7.38	-1.79	0.67	7.62	HOMO-3→LUMO+1(4) HOMO-2→LUMO+2(10) HOMO-1→LUMO+1(18) HOMO→LUMO+1(8) HOMO→LUMO+2(35) HOMO→LUMO+4(4) HOMO→LUMO+5(3)

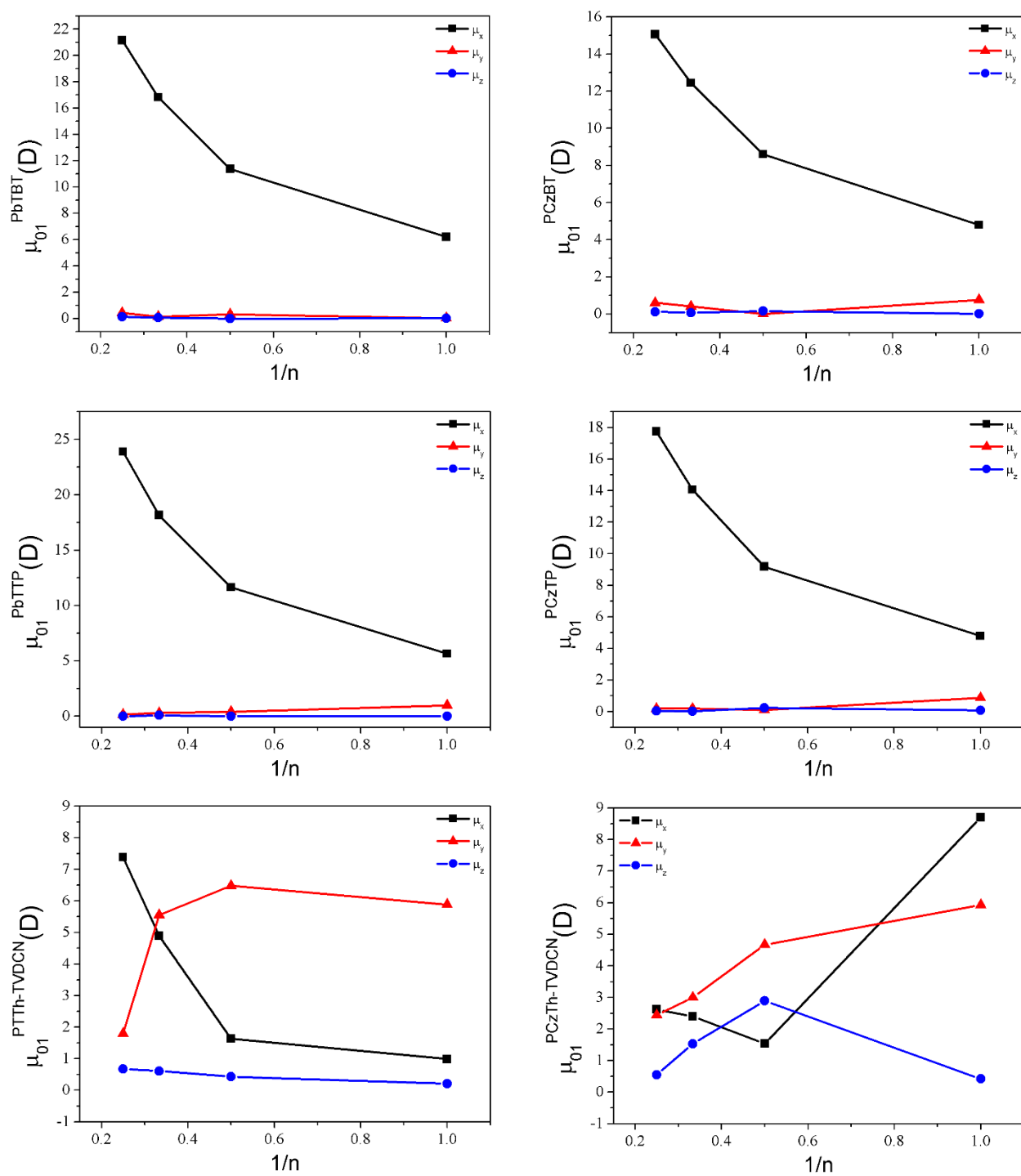


Figure S2. Absolute values of $S_0 \rightarrow S_1$ transition dipole moment as determined with TDDFT at the tuned-LC-BLYP/6-31G(d,p) level of theory.

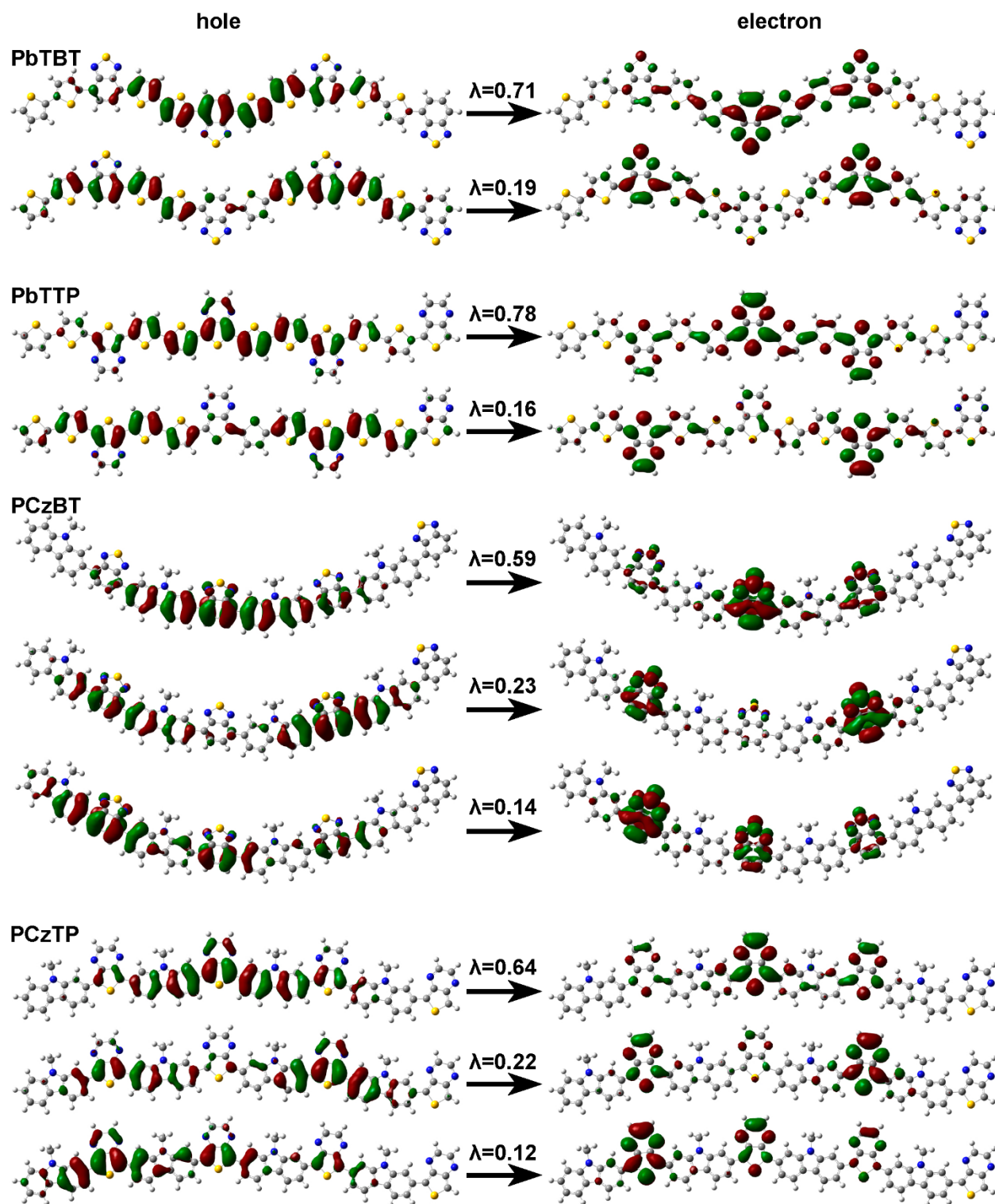


Figure S3. Natural transition orbitals (NTO) describing the $S_0 \rightarrow S_1$ transition for the linear copolymers as determined with TDDFT at the tuned LC-BLYP/6-31G(d,p) level of theory.

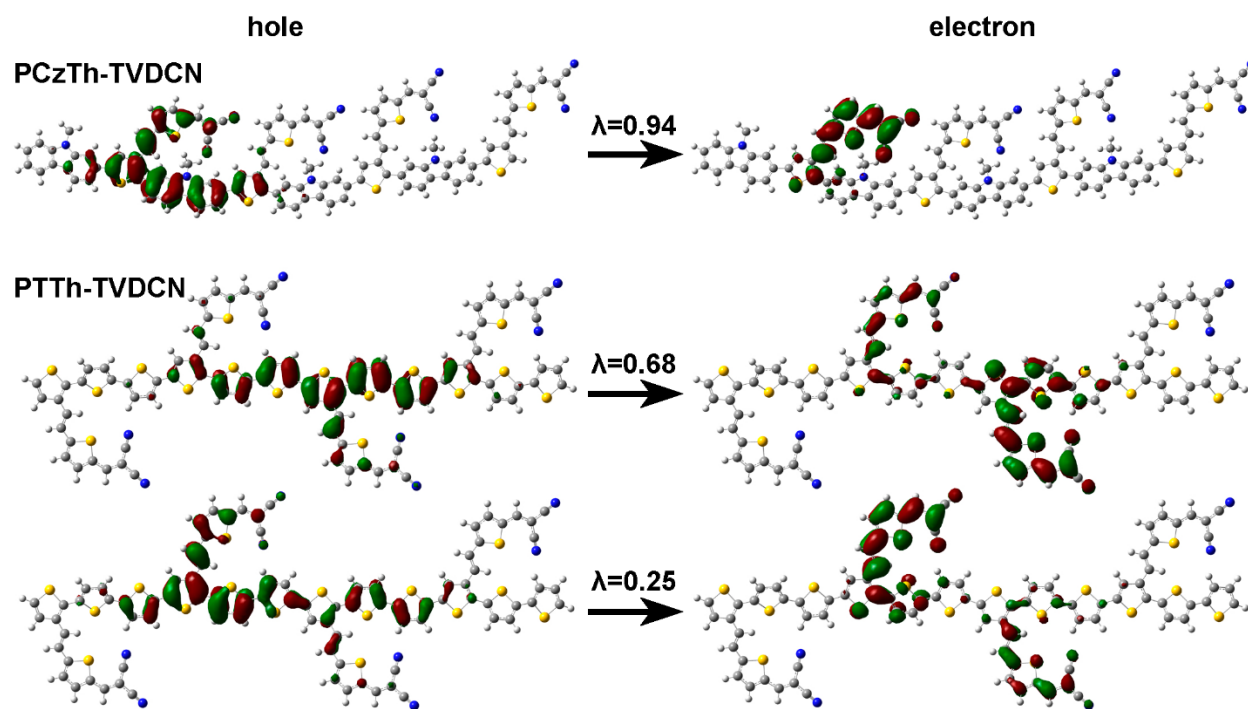


Figure S4. Natural transition orbitals (NTO) describing the $S_0 \rightarrow S_1$ transition for the orthogonally conjugated copolymers as determined with TDDFT at the tuned LC-BLYP/6-31G(d,p) level of theory.

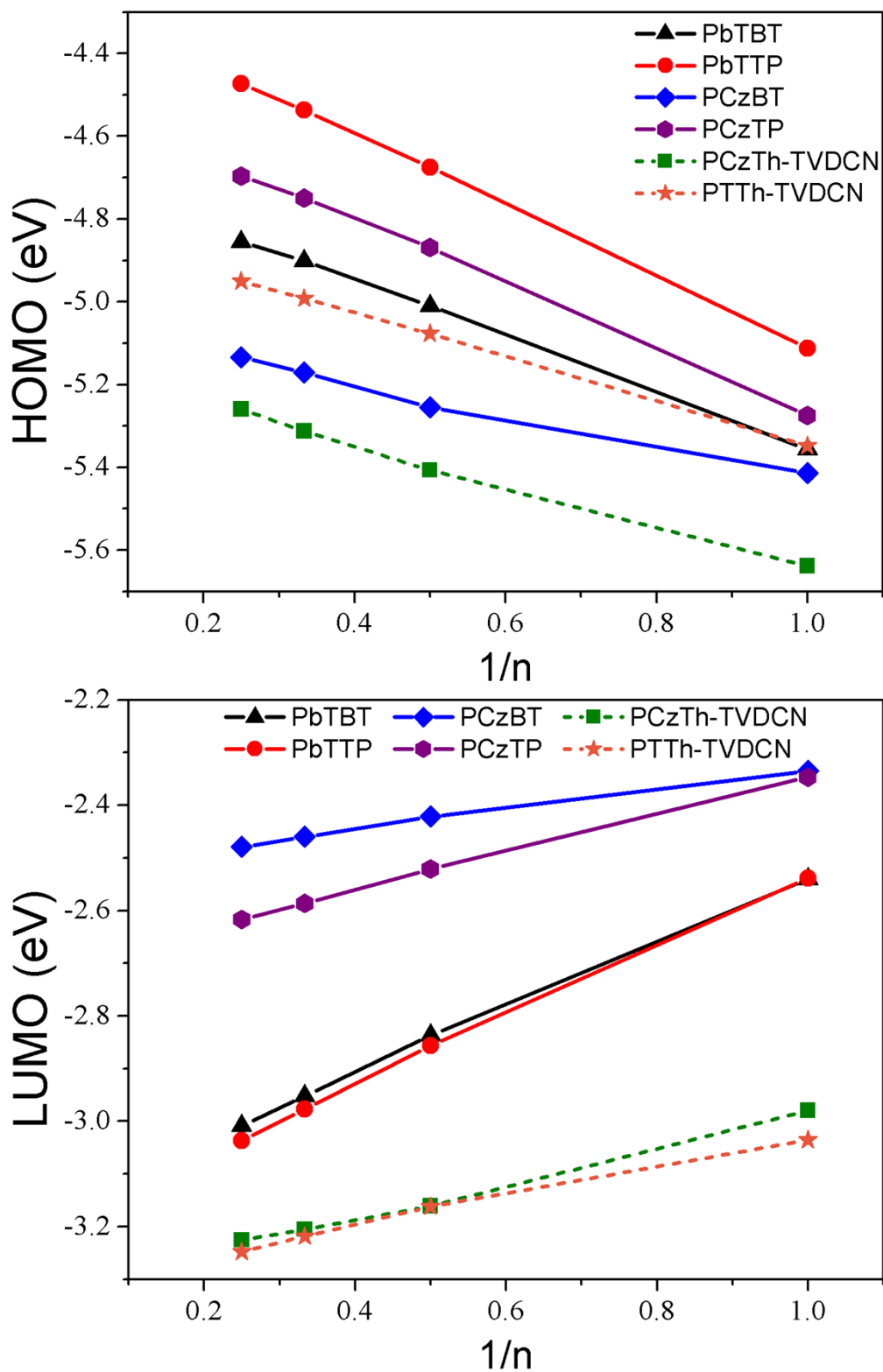


Figure S5. Evolution of the HOMO (top) and LUMO (bottom) energies (eV) with respect to the inverse number of repeat units (n) in the oligomer as determined at the B3LYP/6-31G(d,p) level of theory.

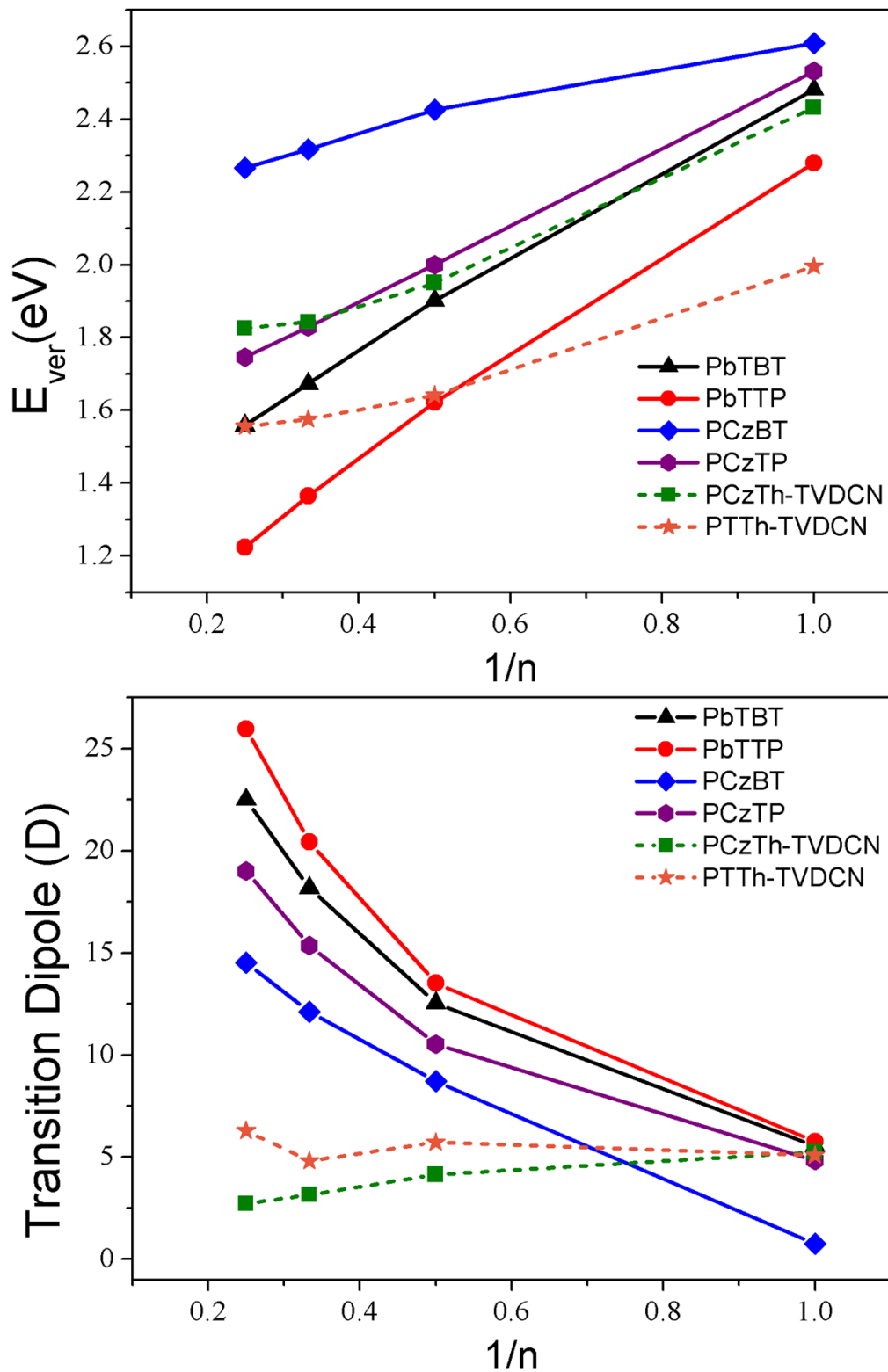


Figure S6. Evolution of the $S_0 \rightarrow S_1$ vertical transition energy (top) and absolute value of the transition dipole moment (bottom) with respect to the inverse number of repeat units ($1/n$), as calculated with TDDFT at the B3LYP/6-31G(d,p) level of theory.

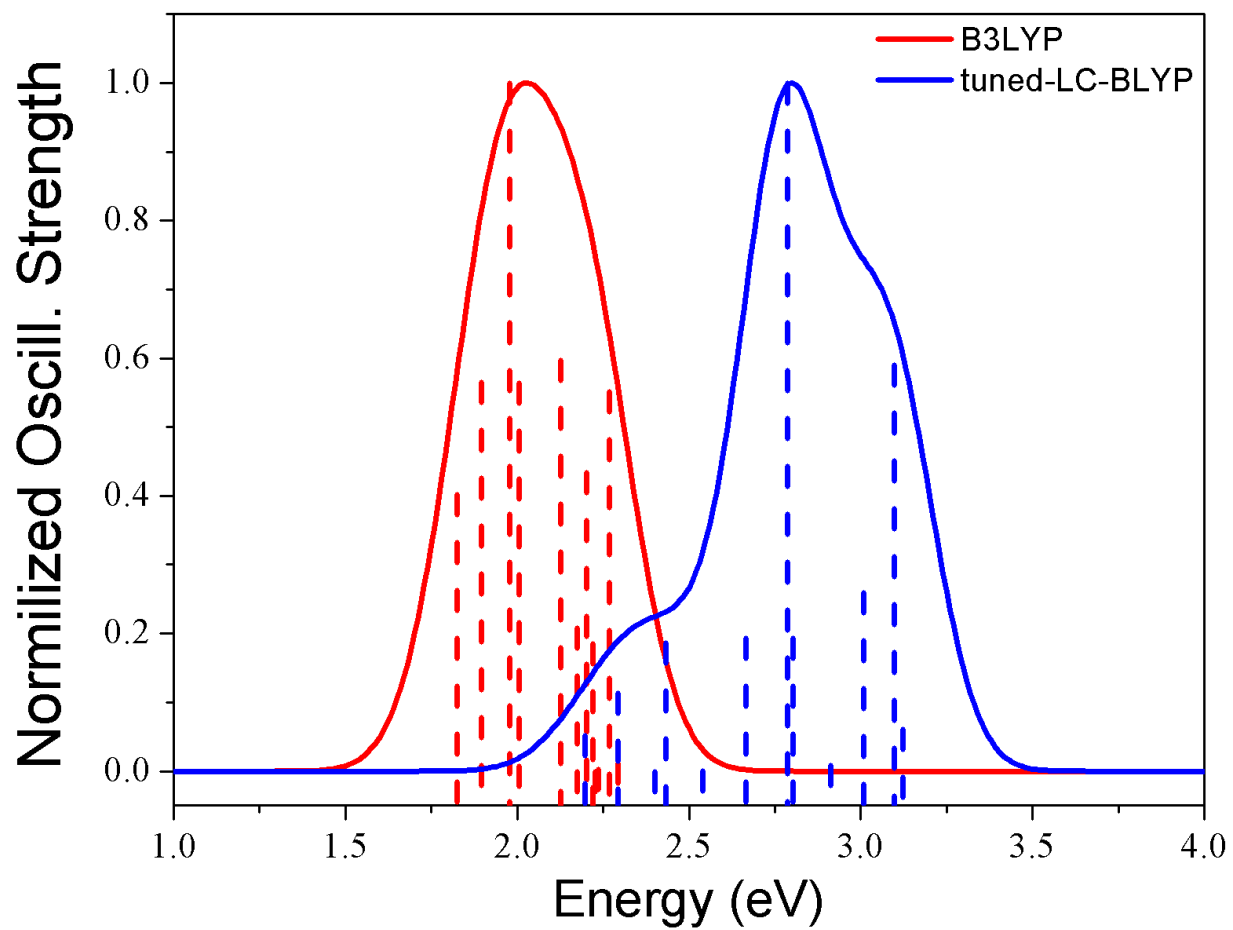


Figure S7. UV-visible absorption spectra of the PCzTh-TVDCN calculated at the B3LYP (red) and tuned-LC-BLYP (blue) both with the 6-31G(d,p) basis set.